LUMINESCENCE INVESTIGATION OF POWDER ZNO NANOPARTICLES DOPED WITH SM AND LI IONS PREPARED BY COPRECIPITATION METHOD

H. Hantour *, N. A. Mohsen *, S. N. El-Sayed *, A. M. A. Mahmoud*

* Faculty of Science, Physics Department, Al-Azhar University (Girls), Cairo, Egypt

ABSTRACT

The present study focuses on the structural and optical properties of ZnO doped with Sm and Li at very dilute concentrations, with compounds $Zn_{1-x-y}Sm_xLi_yO$ (x = 0, 0.03 and y =0, 0.01, 0.03, 0.05). These compounds have been synthesized by a chemical coprecipitation method and characterized by X-ray diffraction (XRD), transmission electron microscopy (TEM) and Raman microscopy. The XRD pattern of all the samples showed ZnO hexagonal wurtzite structure, sharp and intense peaks with small change in lattice parameters due to doping in ZnO, indicating the substitution of Sm and Li ions for Zn sites. For Raman spectra, the strongest peak centered at about 435-437 cm^{-1} can be observed in all the samples, and the intensity of this peak decreases with Sm doping and increases with Li doping. The optical properties of the samples were systematically studied by ultraviolet-visible spectroscopy (UV-V) and photoluminescence (PL) spectroscopy. The maximum absorption of ZnO and $Zn_{0.97}Sm_{0.03}O$ samples appears around 370 and 374 nm respectively near the absorption edge. Doping with Li affects the absorption edge and make it shift toward ultra violet and that the absorption increase with increasing Li content. The PL spectra show a broad and strong visible emission at 564 nm emission covering a large part of the visible region indicating the presence of intrinsic defects like vacancies.

INTRODUCTION

ZnO is one of the most important n-type semiconductor materials with a 3.37 eV band gap at room temperature and 60 meV excitation banding energy and an efficient UV absorber [1-5]. It also shows remarkable potential application in catalysts, electrical and optical devices, varistors, gas sensors and solar cells [6-9], cosmetic materials and so on. In addition, ZnO is nontoxic and environmentally friendly that is valuable for bioapplications [10-11]. ZnO has high transparency in the visible and near-ultraviolet spectral regions and wide conductivity range, it is synthesized by different types of techniques such as sputtering, spray pyrolysis, ball milling method and wet chemical method [12]. Recently, ZnO has been synthesized in various shapes, like nanorods, nanospheres, nanoflowers etc, and doped with rare-earth (RE) ions to obtain enhanced luminescence properties[13-15]. These qualities make the aforementioned structures useful in various optoelectronic devices like vacuum fluorescent display (VFD), field emission display (FED) and electroluminescent display (ELD) [16-18]. The intra-shell transitions between the 4f shells of the RE ions make their luminescence properties very attractive. Doping RE ions into the ZnO matrix is very difficult because, firstly, the ionic radius of Sm^{3+}ion (0.964˚A) is much larger than that of Zn^{2+} ion (0.74˚A) and secondly, substitution creates a charge imbalance. The charge compensation from the local defect sites results in lattice deformation, which is not desired. It would be much more convenient to provide a charge compensating material for the formation of a stable compound like alkali metals Na, K, Li etc. In the case of high temperature treatment, the luminescence efficiency of rare-earth materials is often found to decrease due to self-quenching. That is why room temperature synthetic methods, like precipitation method, sol-gel method, etc. are considered very convenient methods for rare-earth doping [13]. In spite of the numerous studies, not all mechanisms responsible for physical phenomena in ZnO are fully understood. One of the problems concerns the origin of spontaneous emission which has been broadly investigated by photoluminescence (PL) spectroscopy. Typically, the room temperature spectra of ZnO consist of a UV emission and possibly one or more visible bands [19-23]

(violet, blue, green, yellow [24-30], orange or red [31-36]). The origin of the UV peak is well explained because it is related to the near-band-edge excitonic transitions. Whereas the origin of the visible emission is highly controversial and there is still no consensus on the origin of this emission and a number of different hypothesis have been proposed to explain this. For a long time, the origin of the green luminescence has been attributed to the oxygen vacancies or zinc vacancies, or surface defects [37-41]. There are also huge discrepancies between theoretical models of defects in ZnO, different studies predict different energy levels for the same type of defect and, consequently, no constructive conclusions can be made ,the difficulties in identifying the origin of defects bands in ZnO is the fact that the bands are broad and overlapping [42]. The present study focuses on the influence of small concentrations of Sm and Li ions on the structural and optical properties of ZnO nanoparticles.
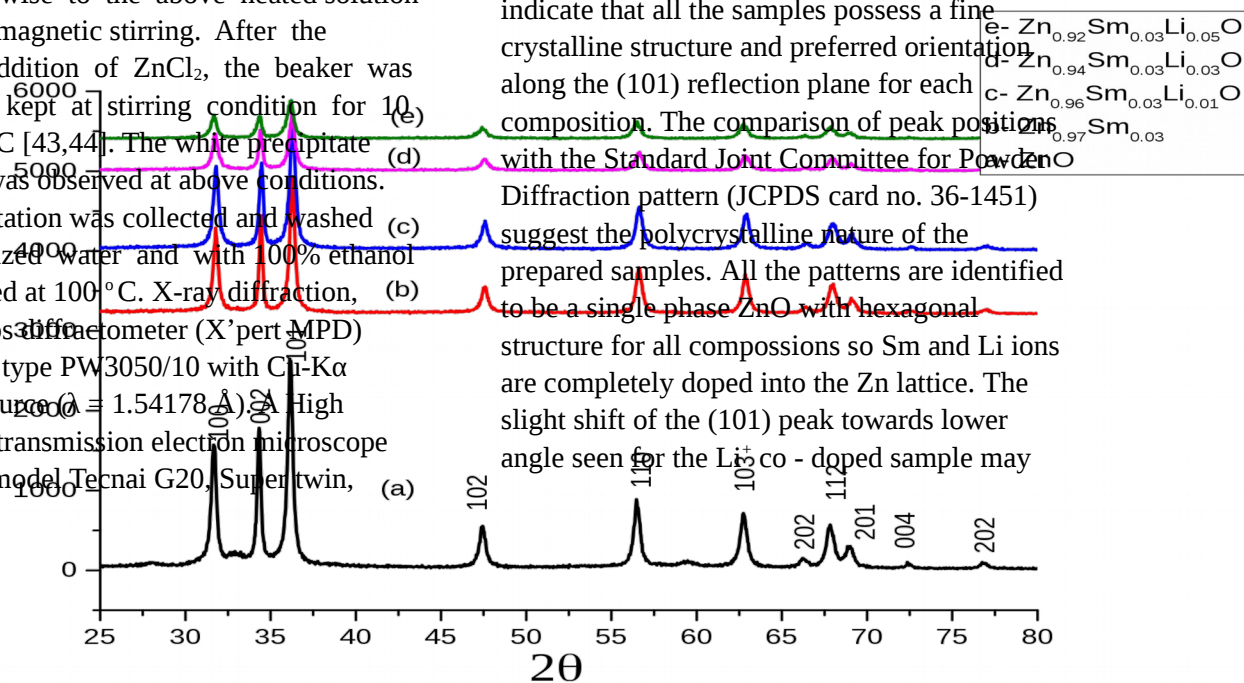
2. EXPERIMENTAL

Samples of powder ZnO nanoparticles doped with different concentrations of Sm and Li ions have been prepared by chemical coprecipitation by mixing an appropriate amount of NaOH, $ZnCl_2$, $SmCl_3$ and $LiSO_4$, that 0.5M aqueous solution of $ZnCl_2$ and 1M of NaOH were prepared in deionized water. 1M of NaOH solution was taken in a beaker and heated to 50° C. After 5 mintes of heating the NaOH solution, $ZnCl_2$ was added dropwise to the above heated solution under high magnetic stirring. After the complete addition of $ZnCl_2$, the beaker was sealed and kept at stirring condition for 10 min at 50° C [43,44]. The white precipitate formation was observed at above conditions. The precipitation was collected and washed with deionized water and with 100% ethanol then air dried at 100° C. X-ray diffraction, using Philips diffractometer (X'pert MPD) goniometer type PW3050/10 with Cu-Kα radiation source ($\lambda = 1.54178$ Å). A High Resolution transmission electron microscope (HRTEM) model Tecnai G20, Super twin,

double tilt with applied voltage: 200 kV and magnification range up to 1,000,000 x and Gun type LaB6, was used to identify the microstructure. Absorbance measurement was carried out by using Perkin-Elmer Spectrophotometer, model lambda 35 in the UV/Visible spectral range. Raman spectrometer (Bruker) was used, the calibration is done automatically by the instrument with Neon lamp. This instrument is characterized by the removal of fluorescence background and high wave number accuracy. The laser wavelength 532-785 nm, laser characteristics (lasing medium) AlGaAs (laser type) semiconductor and the spot size of laser is 20 xobjective $4x10^{-12}(4\mu m^2)$. All spectra were recorded at room temperature under similar spectral parameters. The Perkin Elmer Ls55 florescence spectrometer used to measure Photoluminescence intensity of the samples has holographic gratings to reduce stray light, as well as automated polarizers. Ls55 uses a high energy pulsed xenon source for excitation and has a wide wavelength rang 200- 900 nm.

3. RESULTS AND DISCUSSION

3.1 X-ray diffraction analysis (XRD)

The XRD patterns of the powder samples $Zn_{1-x-y}Sm_xLi_yO$ (x = 0, 0.03 and y=0, 0.01, 0.03, 0.05) at room temperature are shown in **Fig.1**. The XRD study was done over a wide range of Bragg angles (20˚–80˚). The XRD pattern of all the samples showed ZnO hexagonal structure with sharp and intense peaks corresponding to the wurtzite structure of ZnO. The sharp peaks indicate that all the samples possess a fine crystalline structure and preferred orientation along the (101) reflection plane for each composition. The comparison of peak positions with the Standard Joint Committee for Powder Diffraction pattern (JCPDS card no. 36-1451) suggest the polycrystalline nature of the prepared samples. All the patterns are identified to be a single phase ZnO with hexagonal structure for all compossions so Sm and Li ions are completely doped into the Zn lattice. The slight shift of the (101) peak towards lower angle seen for the Li^+ co - doped sample may

e- $Zn_{0.92}Sm_{0.03}Li_{0.05}O$
d- $Zn_{0.94}Sm_{0.03}Li_{0.03}O$
c- $Zn_{0.96}Sm_{0.03}Li_{0.01}O$
b- $Zn_{0.97}Sm_{0.03}$
a- ZnO

indicate an increase in the lattice parameters due to Li$^+$ doping . This increase in lattice parameters is due to lattice distortion as Li$^+$ ions occupy the lattice sites [45]. The refined structural parameters obtained from Rietveld analysis applying the MAUD program. The crystal size of the samples calculated by Debye-Scherrer formula and was found to be in the range 11–14 nm as in **Table1**.

3.2 High resolution transmission electron microscopy (HRTEM)

Results obtained by high resolution transmission electron-microscopy (HRTEM) are shown in **Fig.2** and **Fig.3**. The selected area electron diffraction (SAED) images are shown in Fig.2, these graphs confirm that the ZnO and doped powder is in crystalline wurtzite structure as revealed by the XRD measurements.

3. 3 Raman spectroscopy

In order to investigate the influence of Sm and Li on the vibrational properties of ZnO, Raman scattering study has been performed on pristine and ZnO:Sm samples. **Fig.4** shows the RT Raman spectra of all the samples with the 514 nm line of an argon laser. From Fig.5 the observed peaks of all the samples located at 66-70, 97-99, 212, 328-333, 435-437, 538-554, 579, 990, 1001 and 1086-1088 nm . The peaks located at 331, 379, 438 and 579 cm^{-1} can be assigned to E_{2H} -E_{2L}, $A_{1(TO)}$, E_{2H} and $A_{1(LO)}$ vibration modes of ZnO with P6$_3$mc symmetry [46-50] . The strongest peak centered at about 435-437 cm^{-1} can be observed in all the Raman spectra, and the intensity of this peak decreases with Sm doping. It may be mainly related to the
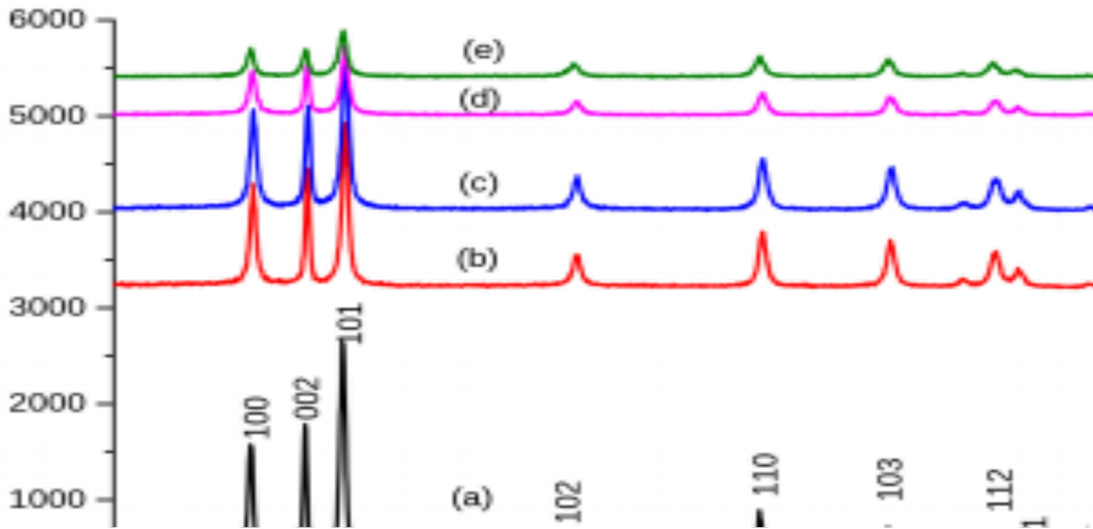

Fig.1 Diffraction patterns of powder samples Zn$_{1-x-y}$Sm$_x$Li$_y$O measured at room temperature (RT)

Table 1 The refined lattice parameters (a and c) (A$^°$), crystallite size (L nm) and mean square strain (ε) obtained from Rietveld analysis of Zn$_{1-x-y}$Sm$_x$Li$_y$O samples at room temperature

Parameter	ZnO	Zn$_{0.97}$Sm$_{0.03}$O	Zn$_{0.96}$Sm$_{0.03}$Li$_{0.01}$O	Zn$_{0.94}y$Sm$_{0.03}$Li$_{0.03}$O	Zn$_{0.92}y$Sm$_{0.03}$Li$_{0.05}$O
a	3.242	3.2445	3.2462	3.2474	3.2493
c	5.192	5.1956	5.1979	5.2045	5.2074
L (nm)	14.1	13.3	12.3	11.5	11.2
ε x 10^{-3}	3.83	2.65	1.34	1.32	1.28

worse crystallization of the doped samples due to the distortion of the crystal lattice in ZnO by RE doping [46]. By farther Li doping the intensity of the peak increase, that increase the goodness of the crystallinty. The band at 435-437 cm^{-1} is attributed to the E_2 high mode of the ZnO single crystalline hexagonal wurtzite structure of ZnO. This band is related to the motion of oxygen atoms and is sensitive to internal stresses. Their presence in all the species reveals their structural stability (ZnO), as consistent from the XRD results. Additionally, a line broadening resulting from the intrinsic defects associated with the O atoms (as the E_2 high mode is related to the vibration of the O atoms only) in the specimens. This phenomena is due to the larger ionic radius of Sm ions, as compared with Zn ions, as new lattice defects are created or intrinsic host lattice defects are activated while Sm^{3+} substitutes at the Zn^{2+} sites [51]. The band at 379-380 cm^{-1} corresponds to the $A_{1\,(TO)}$ and 410 cm^{-1} corresponds to the $E_{1)\,TO)}$ mode, reflecting the strength of the lattice bond. The peaks in the range 574 – 580 cm^{-1} have been assigned to $E_{1\,(LO)}$ and $A_{1(LO)}$ modes and are related to the host defects such as oxygen vacancies (V_O) and zinc interstitials (Zn_i). Compared to pristine ZnO the intensity of peak at 579 cm^{-1} has increased with increasing Sm content which indicates the substitution of Sm in the ZnO host matrix and suggests enhancement in defects. The peak at 97-100 cm^{-1} corresponds to the $E_{2\,(low)}$ fundamental phonons of hexagonal ZnO. The other peaks may indicate multiphonon scattering in pristine and ZnO:Sm samples.

4. OPTICAL PROPERTIES

4.1 Ultraviolet-visible (UV-vis) spectroscopy

The optical absorption spectra of the samples by UV-vis spectrophotometer in the range of 200 to 800 nm were presented. From **Fig.5** it can be seen that the excitonic absorption peak (maximum absorption) of undoped and Sm doped ZnO samples appears around 370 and 374 nm respectively near the visible region .Sm doped ZnO has higher absorption and shifted to higher wavelength than the undoped ZnO. Doping with Li affect the absorption edge and make it shift toward ultra violet region , that the maximum absorption of the samples doped with 0.01, 0.03 and 0.05 Li at around 365, 361 and 356 nm respectively (the UV range is 351-363 nm). The absorption increase with increasing Li content ,the maximum absorption with doping Sm 3% and Li 3%.

4.2 photoluminescence (PL) spectroscopy

PL spectroscopy is an effective technique to detect the presence of defects in semiconductors. The PL emission spectra of the pristine, $ZnO:Sm^{3+}$ and Li^+ co-doped $ZnO:Sm^{3+}$ (under excitation of UV light of 325 nm), are shown in **Fig.6**. The emission spectra show a broad emission covering a large part of the visible region. The occurrence of a broad visible emission indicates the presence of intrinsic defects like vacancies. All samples exhibited a near band edge emission at 382 nm, which is originated from the recombination of free excitons [37] and a strong visible emission at 564 nm is observed, which is considered to be related to the single ionized oxygen vacancy due to the recombination of a photon-generated hole with the single ionized changed state of the defect in ZnO. The broad emission band that shown in the visible region in our samples is due to the superposition of green and yellow emissions. It was reported that the oxygen vacancies responsible for the green emission are mainly located at the surface [37]. The origin of these visible emissions is still highly controversial. Generally, the green emission is typically associated with oxygen vacancy, and the yellow emission is associated with interstitial oxygen. The two different oxygen defects are competing with each other, presenting in the competition of green and yellow bands in PL emission spectra. The intensity of the visible emission for all the samples decreases with Sm and Li doping except for Li 1% sample which exhibit increase of the visible emission.
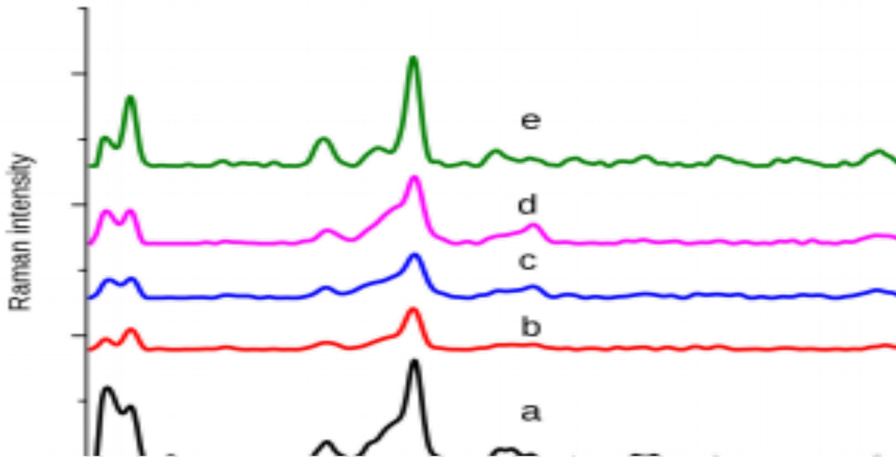
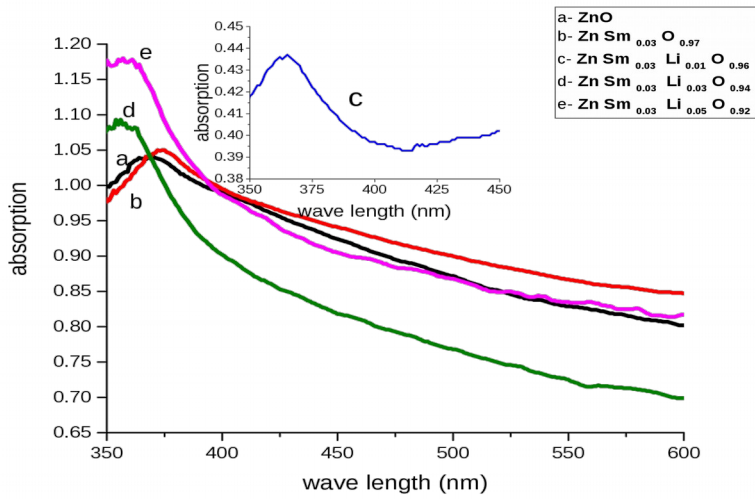**Fig.4 Room temperature (RT) raman spectra of all the samples with the 514 nm line of an argon laser**

a- **ZnO**
b- **Zn Sm** $_{0.03}$ **O** $_{0.97}$
c- **Zn Sm** $_{0.03}$ **Li** $_{0.01}$ **O** $_{0.96}$
d- **Zn Sm** $_{0.03}$ **Li** $_{0.03}$ **O** $_{0.94}$
e- **Zn Sm** $_{0.03}$ **Li** $_{0.05}$ **O** $_{0.92}$

Fig.5   The optical absorption spectra of the samples by UV-vis spectrophotometer in the range of 200 to 800 nm

a- **ZnO**
b- **Zn Sm**
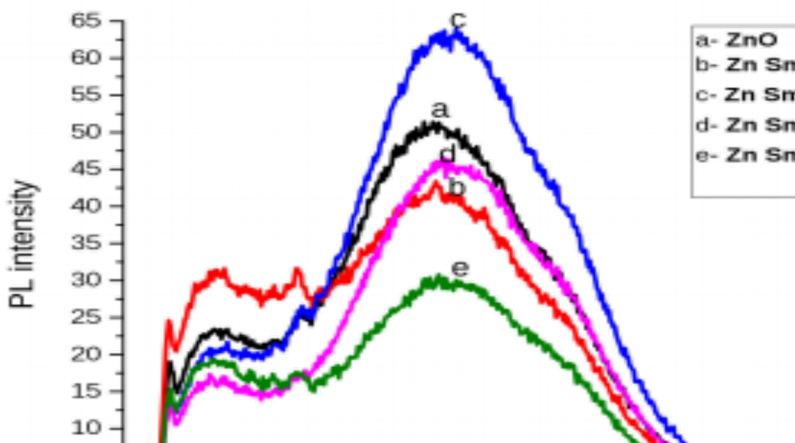c- **Zn Sm**
d- **Zn Sm**
e- **Zn Sm**

Fig.6 The PL emission spectra of   ZnO:Sm:Li samples

CONCLUSION

The powder samples $Zn_{1-x-y}Sm_xLi_yO$ (x = 0, 0.03 and y = 0, 0.01, 0.03, 0.05) have been successfully synthesized by a chemical coprecipitation method , The structural analysis showed that the Sm and Li ions were successfully induced into the ZnO lattice with hexagonal wurtzite structure and no existence of the secondary phases. The detailed optical study of Sm and Li doped ZnO nanoparticles revealed an increase in oxygen defects due to increase in the dopant percentage of Sm and Li. The PL spectra show a broad emission covering a large part of the visible region indicating the presence of intrinsic defects like vacancies.

REFERENCES

[1] H. Soni , Desalination and Water Treatment, 1-8 (2015)

[2] Z.L. Wang, Mater Today 7, 26-33 (2004)

[3] Y.Q. Li, S.Y. Fu, Y.W. Mai, Polymer 47, 2127-2132 (2006)

[4] T. Iwasaki, M. Satoh, T. Masuda, J. Mater. Sci. 35 4025-4029 (2000)

[5] Z. Dang, L. Fan, S. Zhao, Mater. Res. Bull. 38 499-507 (2003)

[6] H. Usui, Y. Shimizu, T. Sasaki, J. Phys. Chem. B 109 120–124 (2005)

[7] Y. Li, G. Li, Q. Yin, Mater. Sci. Eng. B 130 264-268 (2006)

[8] B. Baruwati, D.K. Kumar, Sens. Actuators, B 119 676-682 (2006)

[9] G.C. Yi, C. Wang, W.I. Park, Sci. Technol. 20 S22-S34 (2005)

[10] Z.S. Wang, C.H. Huang, Y.Y. Huang, Chem. Mater. 13 678-682 (2001)

[11] J. Zhou, N.S. Xu, Z.L. Wang, Adv. Mater. 18 2432-2435 (2006)

[12] A.O. Awodugba , Nigerian Journal of Physics 24 102-106 (2013)

[13] P.P. Partha, Nanosystem: Physics, Chemistry, Mathematics, 4: 3 395-404 (2013)

[14] Y. Nakanishi, A. Miyake, Appl. Surf. Sci. 142 233-236 (1999)

[15] M.H. Huang, S. Mao, Science, 292 1897-1899. (2001)

[16] J. Zhang, H. Feng, Ceramics International 33 7 85-788 (2007)

[17] A. Hellemans, Science , 284 2 4-25 (1999)

[18] L. Yi, Y. Hou, Displays, 21147-149 (2000)

[19] A. Karbowski, Nukleonika 58:1189-194 (2013)

[20] AB. Djurisic, Adv. Funct. Mater 14:9 856-864 (2004)

[21] NY Garces, L. Wang, Appl Phys Lett 81:4 622-624 (2002)

[22] Y Gong, T .Andelman, Nanoscale Res Lett 2 297–302 (2007)

[23] L Guo, S Yang, Appl Phys Lett 76 2901-2903 (2000)

[24] L Irimpan, J Appl Phys 102 063524 (2007)

[25] BX Lin, ZX Fu, Appl Phys Lett 79 943-945 (200 1)

[26] X Liu, X Wu, H Cao, J Appl Phys 95:6 3141-3147 (2004)

[27] AK Mishra, SK Chaudhuri, J Appl Phys 102 103514(2007)

[28] CM Mo, YH Li, J Appl Phys 83 4389-4391 (1998)

[29] J Qiu, X Li, Nanotechnology 20:15155603 (2009)

[30] M Ramani, S Ponnusamy, Opt Mat 34817–820 (2012)

[31] FK Shan, GX Liu, Appl Phys Lett 86:221910 Commun 149 550–554 (2008)

[32] F Tuomisto, K Saarinen, Phys Rev B 72 085206 (2005)

[33] D Wang, ZQ Chen, J Appl Phys 107 023524 (2010)

[34] X Wei, B Man, Jpn J Appl Phys, Part 1 458586-8591 (2006)

[35] G Xiong, U Pal, J Appl Phys 101:2 024317 (2007)

[36] QX Zhao, P Klason, Appl Phys Lett 87: 21211912 (2005)

[37] S.Kumar, Nano: Brief Reports and Reviews, World Scientific Publishing Company, 7: 3 1250022 (2012)

[38] U. Koch, A. Fojti , Chem. Phys.Lett . 122 507 (1985)

[39] L. Spa nhel ,J. Am. Chem. Soc.113 2826 (1991)

[40] A. B. Djuris , W. C. H. Choy , Adv.Funct. Mater. 14 856 (2004)

[41] N. S. Norberg, J. Phys. Chem. B 109 20810 (2005)

[42] AB Djurisic, Mat pro and device appl. Prog Quant Electron 34 191-259 (2010)

[43] G.Vijayaprasath, G. Ravi, J. Phys. Chem. C, 118 9715-9725 (2014)

[44] R. Vettumperumal, Materials Research Bulletin 50 7-11 (2014)

[45] L.Sun, C. Qian, Solid State Commun. , 119 393 (2001)

[46] J. Lang, Materials Chemistry and Physics 194 29 -36 (2017)

[47] G. Xiong, U. Pal, J. Appl. Phys. 101 (1-6) 024317 (2007)

[48] L.L. Yang, J.H. Yang, Phys. E 40 920-923 (2008)

[49] A. Kovalenko, G. Pourroy, J. Phys. Chem. C 114 9498-9502 (2010)

[50] J.H. Lang, J.Y. Wang, Mat.Sci. Semicon. Proc. 41 32-37 (2016)

[51] D. Arora , RSC A dv., , 6,78122–78131 (2016)